Int. J. Environ. Sci. Technol. (2016) 13:1319–1328
DOI 10.1007/s13762-016-0970-y

ORIGINAL PAPER

Adsorption of Ag^+ ions on hydrolyzed lignocellulosic materials based on willow, paulownia, wheat straw and maize stalks

P. S. Vassileva[1] · T. Hr. Radoykova[2] · A. K. Detcheva[1] · I. A. Avramova[1] · K. I. Aleksieva[3] · S. K. Nenkova[2] · I. V. Valchev[2] · D. R. Mehandjiev[1]

Received: 24 September 2015 / Revised: 18 February 2016 / Accepted: 20 February 2016 / Published online: 4 April 2016

Abstract In the present work, the adsorption of Ag^+ ions on hydrolyzed plant biomass (willow, paulownia, wheat straw and maize stalks) was investigated. Chemical analyses were performed to establish the composition of the obtained materials. Adsorption mechanism, adsorption sites and specific surface areas of these materials were examined by BET analysis, IR spectroscopy, XPS and EPR. The effects of contact time, acidity of initial solutions and Ag^+ ion concentrations were followed. Pseudo-first-order, pseudo-second-order and intra-particle diffusion models were used to analyze kinetic data. In all cases, the adsorption was significantly affected by the pH value. Different types of adsorption isotherms of Ag^+ ions (either Langmuir or Freundlich) were registered depending on the adsorbing material. The adsorption mechanism is complex, and the process passes through different stages as clustering of Ag^+ ions and formation of elemental Ag. The maximal adsorption capacities varied from 2.05 to 6.07 mg g^{-1}. The obtained results revealed that the examined waste lignocellulosic materials are promising adsorbents for Ag^+ ions.

✉ P. S. Vassileva
pnovachka@svr.igic.bas.bg

[1] Institute of General and Inorganic Chemistry, Bulgarian Academy of Sciences, Acad. G. Bonchev Street, Bl. 11, 1113 Sofia, Bulgaria

[2] University of Chemical Technology and Metallurgy, 8 Kl. Ohridski blvd, 1756 Sofia, Bulgaria

[3] Institute of Catalysis, Bulgarian Academy of Sciences, Acad. G. Bonchev Street, Bl. 11, 1113 Sofia, Bulgaria

Keywords Ag^+ ions · Hydrolyzed lignocellulosic materials · Adsorption equilibrium · Adsorption mechanism

Introduction

Renewable agricultural residues are produced in huge quantities as a waste, and their storage and management create environmental problems. On the other hand, their structure, phase composition, chemical stability, water insolubility and mechanical strength render them suitable for preparing valuable materials for different uses. Agricultural wastes can be applied as biosorbents, directly or after activation (Sumathi et al. 2005; Dias et al. 2007; Ioannidou and Zabaniotou 2007; Nameni et al. 2008; Garcia-Reyes et al. 2009; Gupta et al. 2012; Vassileva et al. 2013; Yuvaraja et al. 2014). The advantages of biosorbents are biodegradability and good adsorption properties due to their morphology and surface functional groups (Ngah and Hanafiah 2008; Ali 2010; Ali et al. 2012). Their application has received much attention in sorption of various pollutants from aqueous media (Ali and Gupta 2007; Foo and Hamed 2009; Angelova et al. 2011; Vassileva et al. 2013). This has stimulated the interest in producing new types of highly effective biosorbents from low-cost raw materials. They are usually agricultural by-products, wood processing materials, residual materials from coal carbonization, etc. (Ahmedna et al. 2000; Shinogi and Kanri 2003; Dias et al. 2007; Vassileva and Detcheva 2010, 2011; Gupta et al. 2013; Gupta and Saleh 2013; Saleh et al. 2011; Saleh and Gupta 2014; Saleh and Gupta 2012). Among them, lignocellulosic materials are subject of increasing interest (Volesky 2001; Gardea-Torresdey et al. 2004; Krishnani et al. 2009; Liu et al. 2013). The adsorption of various

metal ions such as Mn(II), Cu(II), Pb(II), Cd(II), Zn(II), Ni(II) on hydrolyzed lignins is discussed in many publications (Guo et al. 2008; Bumba et al. 2010; Cao et al. 2011; Bukhari et al. 2013; Radoykova et al. 2015). The method for preparation of hydrolyzed lignins has usually influence on their chemical composition, surface functional groups and formation of adsorption sites (Radoykova et al. 2015).

The increased interest in bioethanol production from vegetal raw materials poses the question for utilization of the waste hydrolyzed lignin admixed with cellulose. The large internal surface area of the lignocellulosic material and the availability of different functional groups that could act as adsorption sites open the possibility of using such materials as adsorbents for metal ions from aqueous solutions. Most probably coordination bonds are formed between the metal ions and adjacent chains of OH-groups of the lignocellulosic components. No data concerning the adsorption of Ag^+ ions on this type of materials have been reported in the literature. On the other hand, it is known that silver ions have antibacterial activity. It can therefore be assumed that the lignocellulosic carrier with adsorbed Ag^+ ions on its surface can be used as a base for preparation of promising silver-modified catalytic materials for removal of toxic substances from physiologic solutions.

The aim of the present study was to investigate the adsorption properties of waste lignocellulosic materials with respect to Ag^+ ions from aqueous solutions and to throw light on the sorption mechanism and the role of surface functional groups in this process.

These studies were carried out in the period from 2014 to 2015 at the Institute of General and Inorganic Chemistry of the Bulgarian Academy of Sciences (adsorption studies and XPS analysis); the University of Chemical Technology and Metallurgy (synthesis and characterization of the adsorbents); and the Institute of Catalysis of the Bulgarian Academy of Sciences (EPR studies) in Sofia, Bulgaria.

Materials and methods

Sample preparation

In the present study, we used hydrolyzed plant biomass from willow, paulownia, wheat straw and maize stalks (denoted as w, p, s and m, respectively) as raw materials.

Technical hydrolyzed lignin (THL) was produced by high-temperature hydrolysis of softwood and hardwood chips to sugars catalyzed by diluted sulfuric acid under factory conditions. The products were further subjected to yeast fodder production. THL was washed and milled. The 0.1- to 0.3-mm sieve fraction was used.

The samples pHL(w) and pHL(p) were obtained by steam explosion treatment for hydrolysis facilitation, followed by enzymatic hydrolysis of willow and paulownia, respectively, with cellulase enzyme complex combined with β-glucosidase. The steam explosion was performed in a 2-L stainless steel laboratory installation at a hydromodule ratio of 1:10; initial temperature 100 °C; maximal temperature 190 °C; pressure 12.8 bar; heating time 60 min; and time at maximal temperature 10 min. The enzymatic hydrolysis was carried out in polyethylene bags in a water bath preheated to the desired temperature under the following conditions: temperature 50 °C, reaction time 24 h, lignocellulose content 10 %, $pH_{initial}$ 5.5–6.0, pH_{final} 4.2–4.6 and 5 % charge of the cellulase enzyme complex NS 22086 in combination with 0.5 % β-glucosidase NS 22118 (Novozymes AS). Both percentages refer to the mass. All amounts and experimental conditions were according to the Novozymes Application Sheet.

The samples hHL(s) and hHL(m) were obtained by hydrothermal treatment for hydrolysis facilitation, followed by enzymatic hydrolysis of wheat straw and maize stalks, respectively, with cellulase enzyme complex combined with β-glucosidase. The hydrothermal hydrolysis of the agricultural lignocellulosic raw materials was performed in 1000-mL stainless steel laboratory autoclaves rotated at a constant rate under the following conditions: biomass/water ratio of 1:10; initial temperature 100 °C; maximal temperature 190 °C; heating time 60 min; and time at maximal temperature 30 min. Enzymatic treatment conditions were as follows: temperature 50 °C, reaction time 72 h, lignocellulose content 10 %, $pH_{initial}$ 5.5–6.0 and 5 % charge of the cellulase enzyme complex NS 22086 in combination with 0.5 % β-glucosidase NS 22118.

Sample characterization

The porous structure of the studied samples was investigated by low-temperature (−196 °C) nitrogen adsorption using a Quantachrome Nova 1200 apparatus. Prior to nitrogen adsorption, the samples were degassed at 300 °C for 3 h. Specific surface area was calculated on the basis of the BET equation.

The cellulose content in the studied lignocellulosic materials was determined according to Obolenskaya et al. 1965, the lignin content—according to (acid-insoluble lignin in wood and pulp, TAPPI standard test method T 222 om-11) and the ash amount—according to (ash in wood, pulp, paper and paperboard: combustion at 525 °C, TAPPI standard T 211 om-02).

Elemental analyzer EuroVector EA 3000 was used for analysis of C, N, S and H. The oxygen content of the samples was calculated by the difference of the total sum of

carbon, hydrogen, nitrogen, sulfur and ash contents from 100 %.

The EPR measurements were taken at room temperature on a JEOL JES-FA 100 spectrometer operating in the X-band range. Standard cylindrical cavity TE_{011} was used. The powder samples were placed in quartz tubes and measured.

The infrared spectra were recorded on a Varian 660 IR spectrometer. For preparation of the KBr pellets, the samples were ground in an agate mortar.

The XPS study was carried out by means of ESCALAB MKII spectrometer with Al Kα (unmonochromatized) source at 1486.6 eV with a total instrumental resolution of ~1 eV, under base pressure of 10^{-8} mbarr. The C1*s*, O1*s*, N1*s*, Ag3*d* and Si2*p* photoelectron lines were recorded and calibrated with respect to the C1*s* line at 285.0 eV. XPSPEAK 4.0 fitting program was used for deconvolution of the photoelectron peaks. All data were recorded at a 45° takeoff angle.

Adsorption studies

Stock standard solution (1000 mg/L) of the Ag^+ ions was prepared (Titrisol, Merck, Germany) and correspondingly diluted to obtain the various preset initial concentrations. Adsorption experiments were carried out at 20 ± 1 °C in the batch mode. Experiments were carried out using stoppered 50-mL Erlenmeyer flasks containing about 0.2 g of the sample and 20 mL of the aqueous solution of Ag^+ ions. The suspensions were shaken on a rotary shaker at 150 rpm. In order to optimize the contact time for the adsorption, kinetic experiments were carried out. The adsorption was studied at different time intervals varying from 2 min to 24 h. Kinetic adsorption experiments were performed using solutions with initial ion concentration of 75 mg/L (pH 5.1). After reaching equilibrium, the adsorbent was removed by filtration through a Millipore filter (0.2 μm). The initial and equilibrium concentrations of the Ag^+ ions were determined by flame AAS on a Pye Unicam SP 192 flame atomic absorption spectrometer (UK). Measurements by flame AAS were taken at the most sensitive wavelength of Ag (328.1 nm) using an air/acetylene flame under standard operating conditions. The calibration solutions were prepared by stepwise dilution of the stock standard solution.

The effect of acidity on the efficiency of the studied adsorbents was investigated over the pH range from 1.5 to 5.1 (pH-meter model pH 211, Hanna instruments, Germany), employing an initial Ag^+ concentration of 75 mg/L. The initial solution pH was adjusted using 0.1 M HCl or 0.1 M NaOH. In order to determine the effect of the initial metal ion concentrations on the adsorption capacity, initial concentrations in the range of 5–75 mg/L at pH 5.1 were chosen.

Analytical purity grade reagents were used in all experiments. All adsorption experiments were replicated, and the average results were used for data processing.

The amount of Ag^+ ions adsorbed by the examined samples at equilibrium (Q_e, mg/g) was calculated using the expression:

$$Q_e = (C_0 - Q_e) \times \frac{V}{m} \quad (1)$$

where C_0 and C_e are the initial and equilibrium concentrations of Ag^+ (mg/L), respectively. V is the solution volume (in liters L), and m is the adsorbent mass (g).

Results and discussion

Chemical composition and specific surface area

The studied lignocellulosic materials contain lignin and polysaccharides, strongly connected to the latter and resistant to hydrolysis. In Table 1, the data for the chemical compositions and the specific surface areas of the

Table 1 Chemical composition and specific surface area data of the investigated hydrolyzed materials

Hydrolyzed materials	THL	pHL(p)	pHL(w)	hHL(s)	hHL(m)
Chemical composition					
Mineral substances (%)	9.1	3.4	2.7	6.5	6.9
Cellulose (%)	12.8	58.6	52.3	50.4	50.6
Lignin (%)	78.0	37.4	44.1	42.9	41.9
Elemental composition					
C (%)	58.6	58.7	54.9	48.3	48.0
H (%)	6.3	6.6	6.3	6.2	6.0
N (%)	–	0.9	0.6	0.6	0.9
S (%)	0.7	–	–	–	–
O (%)	25.3	30.5	35.5	38.4	38.2
Surface area, $m^2\ g^{-1}$	15.8	12.0	15.2	10.5	10.0

investigated materials are presented. The data show that the samples differ substantially in regard to the lignin and cellulose contents. The highest lignin content is manifested by sample THL—78 %, and it is lower for the other samples, changing slightly from 37.1 for pHL(p) to 44.1 % for pHL(w). Concerning the cellulose content, the lowest amount is observed for THL—12.8 %, while it is higher for the other samples, changing slightly from 50.4 for hHL(s) to 58.6 for pHL(p). The carbon, hydrogen and oxygen contents in all samples do not substantially differ from one another. Only THL contains sulfur because of the use of sulfuric acid as catalyst in the hydrolysis process, and contains no nitrogen. The specific surface area data vary from 10.0 to 15.8 $m^2\ g^{-1}$, which are sufficiently high for these types of materials.

The lignocellulosic materials, obtained after hydrolysis of wood biomass [THL, pHL(w) and pHL(p)], contained the highest amounts of carbon. The samples, obtained after hydrolysis of wheat straw and maize stalks [hHL(s) and hHL(m)], contained the highest amounts of oxygen and the lowest amounts of carbon. Based on these observations, it may be assumed that the structures of hHL(s) and hHL(m) are condensed on a smaller scale and contain a larger number of free groups.

Adsorption studies

Kinetic studies

The effect of contact time on the amount of adsorbed Ag^+ ions is presented in Fig. 1a. The adsorption increases with the increase in agitation time and reaches a maximal value within 15 min for all studied materials. This short-time interval required to attain equilibrium implies an excellent affinity of the investigated adsorbents toward the silver ions in an aqueous solution. Nevertheless, all further experiments were performed at a contact time of 2 h for certainty.

In order to determine the rate-controlling step in the mechanism of the adsorption process, two kinetic models were applied to the experimental data. The pseudo-first-order (Leinonen and Letho 2001) and pseudo-second-order (Ho and Mckay 1999) rate equations are as follows:

$$\log(Q_e - Q_t) = \log Q_e - \left(\frac{k_1}{2.303}\right)t \quad (2)$$

$$\frac{t}{Q_t} = \left(\frac{1}{k_2 Q_e}\right) + \left(\frac{1}{Q_e}\right)t \quad (3)$$

where Q_t amount of Ag^+ ions adsorbed after a certain time t (mg/g) and k_1 rate constant of pseudo-first-order adsorption (1/min), Q_e equilibrium adsorption capacity (mg/g) and k_2 rate constant of pseudo-second-order adsorption (g/mg min).

Table 2 shows the kinetic parameters for the Ag^+ adsorption process on all studied lignocellulosic materials. The theoretical Q_e values calculated from the pseudo-first-order kinetic model differ from the experimentally measured ones, and the corresponding correlation coefficients are lower than those for the pseudo-second-order model (Table 2). On the other hand, the theoretical values obtained based on the pseudo-second-order kinetic model are very close to the experimental Q_e values. Thus, we concluded that Ag^+ adsorption could be more accurately described by the pseudo-second-order kinetic mechanism.

The intra-particle diffusion model was considered in order to determine the participation of diffusion mechanisms during the adsorption of silver ions by the studied materials. In this model, the rate of intra-particle diffusion is a function of $t^{1/2}$ and it can be defined by Eq. (4) (Allen et al. 1989)

$$Q_t = k_{id} t^{\frac{1}{2}} + C \quad (4)$$

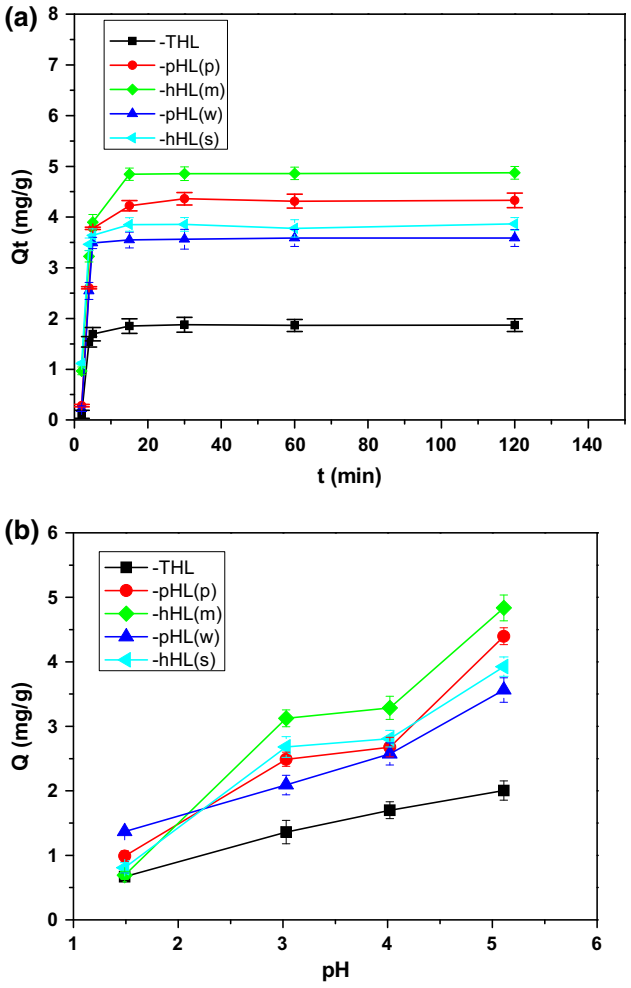

Fig. 1 Effect of **a** contact time and **b** pH on the adsorbed amount of Ag^+ ions on the investigated lignocellulosic materials

Table 2 Kinetic parameters of adsorption of Ag^+ ions onto the investigated hydrolyzed materials

Samples	Pseudo-first-order constants			Pseudo-second-order constants			Intra-particle diffusion constants		
	Q_e (mg/g)	k_1 (1/min)	r^2	Q_e (mg/g)	k_2 (g/mg min)	r^2	k_{id} (mg/g $min^{1/2}$)	C (mg/g)	r^2
THL	0.75	0.032	0.881	1.88	2.133	0.9999	1.84	0.003	0.9784
pHL(w)	1.04	0.028	0.7875	3.61	1.589	1.0000	3.57	0.006	0.8458
pHL(p)	2.74	0.035	0.9483	4.38	0.906	1.0000	4.18	0.015	0.9254
hHL(s)	2.53	0.068	0.9351	3.87	2.582	0.9999	3. 84	0.002	0.9985
hHL(m)	2.84	0.036	0.8787	4.93	0.941	1.0000	4.83	0.004	0.9849

Table 3 pH values of the initial and final solutions

C_0 (mg/L)	Sample									
	THL		pHL(w)		pHL(p)		hHL(s)		hHL(m)	
	pH_0	pH_{final}	pH_0	pH_{final}	pH_0	pH_{final}	pH_0	pH_{final}	pH_0	pH_{final}
5	5.12	2.78	5.12	3.27	5.12	3.50	5.05	3.56	5.12	3.58
25	5.05	2.82	5.05	3.35	5.05	3.47	5.05	3.67	5.05	3.47
50	5.05	2.88	5.05	3.30	5.05	3.32	5.07	3.63	5.05	3.60
75	5.07	2.78	5.12	3.18	5.07	3.30	5.12	3.52	5.07	3.56

where C intercept and k_{id} intra-particle diffusion rate constant (mg/g $min^{1/2}$). According to Eq. (4), a plot of Q_t versus $t^{1/2}$ should be a straight line with a slope k_{id} when the adsorption mechanism is governed by intra-particle diffusion. A plot of Q_t versus $t^{1/2}$ would give a straight line if interlayer diffusion is the rate-limiting process. If the plots do not pass through the origin, the intra-particle diffusion is not the only rate-limiting step, so some other kinetic models can also be simultaneously applied to the adsorption rate.

The presence of two linear sections indicates that the first linear part of the plot (not presented here) corresponds to external mass transfer or film diffusion, whereas the second part of the plot indicates the diffusion into the adsorbent particles passing through the interlayer space (Aksu and Kabasakal 2004; Rida et al. 2013). The intercept value C gives information about the thickness of the boundary layer. The larger the intercept, the greater is the boundary layer effect. The values of k_{id} and C are presented in Table 2.

The correlation coefficients for the intra-particle diffusion model had lower values than those for the pseudo-second-order kinetic model. These results confirmed that the pseudo-second-order mechanism is predominant in the case of adsorption of Ag^+.

Effect of pH on adsorption efficiency

The amounts of adsorbed Ag^+ ions onto the studied materials as a function of pH of the initial solutions are presented in Fig. 1b. The effect of pH was studied in the pH range from 1.5 to 5.1. The pH was limited to values about 5 for avoiding silver precipitation in the form of AgOH or Ag_2O at higher pH values. Silver is present only in the form of Ag^+ in the solution in the studied pH range. As it was expected, the adsorption of Ag^+ ions strongly depends on the acidity of the initial solutions. With the increase in pH, the amount of adsorbed ions increases and the optimal pH range is found out to be above 5.0. It is known that the increase in pH decreases the competition between the hydroxonium and metal ions for surface sites and results in increased uptake of metal ions by the adsorbents. The increase in metal uptake by adsorbents of different types due to increasing pH of solution has been reported by several authors (Detcheva et al. 2011; Gupta et al. 2011a, b; Saleh 2015a, b).

Table 3 presents the pH values of the initial and final solutions, depending on the Ag concentrations. The adsorption process resulted in a decrease of the pH values, which proved that the concentration of H^+ ions in the final solutions is increased. This could be related to a possible ion exchange mechanism of the adsorption process, where Ag^+ ions replace the H^+ ions in the OH-groups on the adsorbents' surface.

Adsorption isotherms

Experimental adsorption isotherms of the investigated materials are presented in Fig. 2. Best adsorption properties are exhibited by the material hHL(m), while the material THL shows the lowest adsorption efficiency, despite its highest specific surface area. THL contains more condensed polymeric structures in its composition in

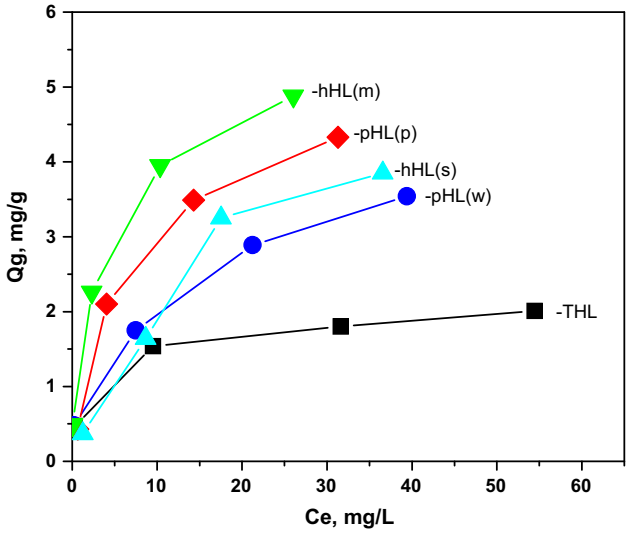

Fig. 2 Adsorption isotherms of Ag^+ ions onto investigated materials

comparison with the other studied materials. The acidic and hydrolyzing effects of the catalyst change the original three-dimensional lignin structure which becomes more complicated and dense, and on its turn leads to low reactivity (Radoykova et al. 2013).

The amount of adsorbed Ag^+ ions for the studied lignocellulosic materials increases in the order:

$$\text{THL} < \text{pHL(w)} < \text{hHL(s)} < \text{pHL(p)} < \text{hHL(m)} \quad (5)$$

No direct relationship was found between chemical composition, specific surface area and adsorption capacity. It can be assumed that the adsorption most probably follows an ion exchange mechanism, which is in agreement with silver adsorption on alfalfa biomass, described by Herrera et al. (2003).

The concentration variation method was used to calculate the adsorption characteristics of both the adsorbent and the process. The adsorption data were analyzed with the help of the following linearized forms of Langmuir and Freundlich types of isotherms:

$$\text{Langmuir isotherm}: \quad \frac{C_e}{Q_e} = \frac{1}{K_L Q_0} + \frac{C_e}{Q_0} \quad (6)$$

$$\text{Freundlich isotherm}: \quad \ln Q_e = \ln k_F + \frac{1}{n} \ln C_e \quad (7)$$

where C_e equilibrium concentration of metal ions (mg/L), Q_e amount of ions adsorbed (mg) per unit of mass of the adsorbent (g), Q_0 adsorption capacity (mg/g), K_L Langmuir constant, k_F Freundlich constant, n intensity of adsorption.

The values of Langmuir and Freundlich parameters were obtained, based on the linear correlation between the values of (1) (C_e/Q_e) and C_e and (2) ln Q_e and ln C_e, respectively (Table 4).

The Langmuir type of model is based on the assumption that all adsorption sites are "equally active," the surface is energetically homogeneous, and a monolayer surface coverage is formed without any interaction between the adsorbed molecules. The Freundlich type of model is valid for heterogeneous surfaces and predicts an increase in the concentration of the ionic species, adsorbed on the surface of the solid when the concentration of certain species in the liquid phase is increased (Vassileva and Detcheva 2010, 2011; Saleh 2015a, b).

The correlation coefficients r^2 (>0.99) proved that the linear fit to the Langmuir type of model was excellent for the studied materials THL and pHL(p), while for pHL(w) and hHL(m) the Freundlich model was more adequate in describing the adsorption processes. The mechanism of Ag^+ adsorption on the material hHL(s) cannot be directly attributed to the Langmuir or Freundlich models (the r^2 values imply that both isotherm models provide good correlations for the adsorption of the silver ions). In any case, the procedure of sample preparation cannot be related to a certain specific type of adsorption isotherm.

It can therefore be concluded that in case of the materials THL and pHL(p) there are no interactions between the adsorbed ions; the adsorption process takes place in a single layer; and the adsorption heat is constant. On the other hand, in case of the materials hHL(m) and pHL(w) there are interactions between the adsorbed Ag^+ ions and the adsorption sites are distributed exponentially with respect to the heat of adsorption.

Table 4 Values of Langmuir and Freundlich parameters for Ag^+ adsorption on the hydrolyzed lignocellulosic materials

Adsorbents	Langmuir parameters			Freundlich parameters		
	Q_0 (mg/g)	K_L (L/mg)	r^2	k_F ($mg^{1-n}L^n g^{-1}$)	n (L/mg)	r^2
THL	2.05	0.409	0.9930	0.70	3.53	0.9648
pHL(w)	3.88	0.183	0.9436	0.84	2.57	0.9969
pHL(p)	5.29	0.142	0.9967	0.96	1.65	0.9188
hHL(s)	4.15	0.151	0.9252	0.89	1.38	0.9686
hHL(m)	6.07	0.497	0.9828	1.56	2.68	0.9937

Mechanism of adsorption of Ag^+ ions

The IR spectral data on the hydrolyzed lignocellulosic materials before and after adsorption of Ag^+ ions were also investigated. It is difficult to estimate the coordinate bonds between Ag^+ and the surface functional groups of the studied materials. The presence of different functional groups, such as –OH, COOH, and –C–O–C–, makes the shape of spectral bands broader and more complex due to the hydrogen bonds and the conformational structure of the materials. In the range of stretching vibrations of –OH 3500–3100 and >C=O 1690–1720 cm^{-1}, the intensity of the bands slowly increased after adsorption of Ag^+ ions, as observed by Saleh and Gupta (2012). These results were expected, because of the hydrogen bonds and the physical interaction of Ag^+ ions with the components of lignocellulosic materials. The shape and shifting of the bands did not change considerably. For these reasons, the intensity of –OH and >C=O stretching bands can be used for qualitative determination of the adsorption of Ag^+ ions by the lignocellulosic materials, as reported by Saleh (2011, 2015).

Ag^+ ion is diamagnetic with filled-up $4d^{10}$ electronic configuration, and it does not exhibit any EPR spectrum. Some of the silver species are paramagnetic: Ag^0 (with the $4d^{10}5s^1$ electronic configuration), Ag^{2+} (with the $4d^9$ electronic configuration), as well as some silver clusters. The g factor of Ag^0 is reported to be isotropic and close to the free electron value of 2.0023, while signals attributed to Ag^{2+} occur at $g\perp \sim 2.05$ and $g\| \sim 2.35$. Aggregation of Ag^0 and Ag^+ ions may additionally generate chemically stable Ag_y^{x+} clusters such as Ag_2^+, Ag_3^{2+}.

Figure 3 shows the EPR spectra of the studied samples. As can be seen, for all samples, a narrow singlet line with g factor 2.0026 is recorded, which is due to Ag^0 (Dhabekar et al. 2006). In sample hHL(m), a broad singlet line with g factor 2.0258 is detected, due to the silver clusters of type Ag_y^{x+} (Baldansuren and Roduner, 2009). In addition, EPR lines are detected in all samples at g factors 4.1224 and 2.1816, attributed to Fe^{3+} ions in tetragonal and octahedral environment, respectively. It follows from the obtained results that the adsorption of silver ions on different samples takes place through a complex mechanism in which phases are defined as silver clusters of type Ag_y^{x+}, and clusters of metallic silver are formed as a final phase in all samples.

Tables 5 and 6 and Fig. 4 present the XRS results for the investigated materials after Ag^+ adsorption. Applying surface-sensitive techniques such as XPS, it is useful to examine the carbon and oxygen XPS spectra of various organic materials to determine the type and relative amount of chemical groups on their surfaces. In most organics XPS spectra, we would expect to find four functional groups and the presence of more than one, relative to one another, would

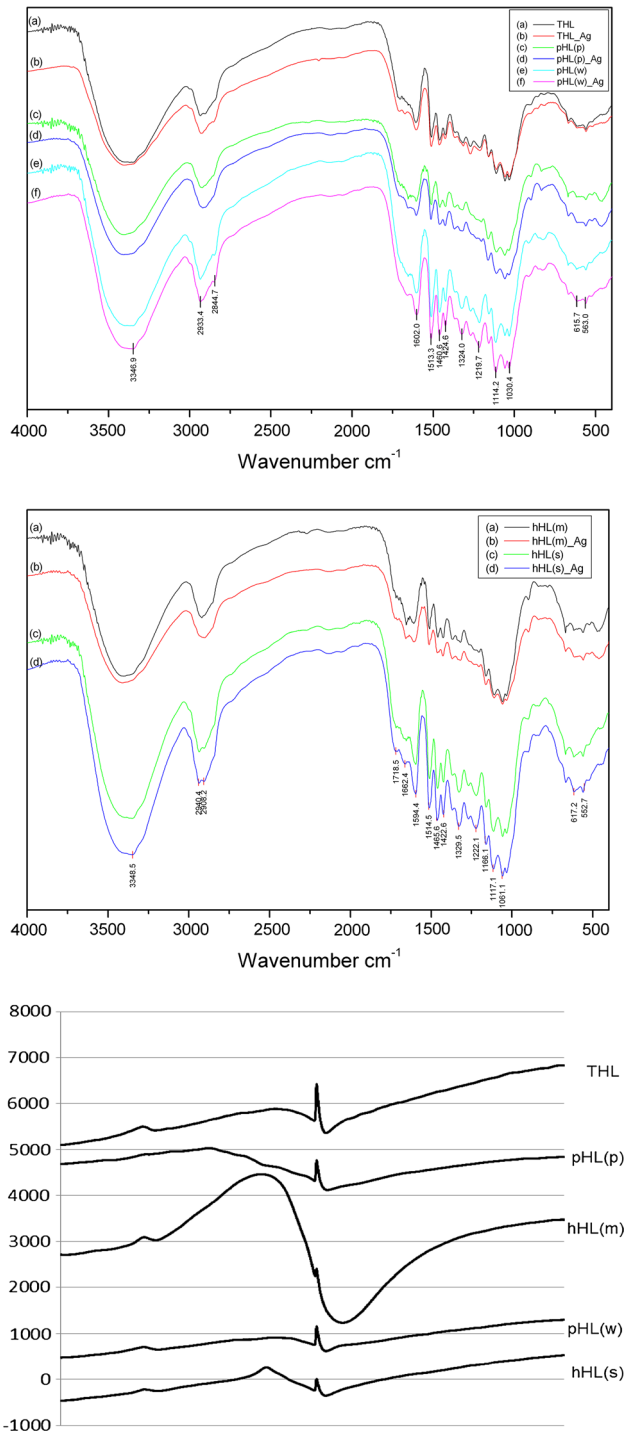

Fig. 3 IR and EPR spectra of the studied samples

be evidence of a chemical change on the surface. The surfaces of the organics were studied before and after adsorption of Ag^+. Evidence for these modifications is given by the changes in the C1*s* photoelectron spectra. The results of C1*s* photoelectron spectra concerning the materials modified by Ag^+ ions are presented in Fig. 4. In order to gain insight

Table 5 Atomic surface concentration of constituent elements in the studied samples

Sample	C (at.%)	O (at.%)	N (at.%)	Si (at.%)	Ag (at.%)	O/C
THL + Ag	72.16	27.72	–	–	0.12	0.38
pHL(p) + Ag	63.78	31.85	4.12	–	0.25	0.49
hHL(m) + Ag	69.57	25.19	1.85	3.35	0.04	0.36
pHL(w) + Ag	75.8	22.9	1.16	–	0.14	0.30
hHL(s) + Ag	66.69	28.04	1.60	3.21	0.18	0.42

Table 6 Calculated amounts of carbon functional groups present on the surface of waste lignocellulosic materials after adsorption of Ag^+ ions

Sample	Carbon, functional groups (%)			
	C1, C–C	C3, C=O	C2, C–O or/and OH	C4, O–C=O
THL + Ag	61.5	8	28.8	1.7
pHL(p) + Ag	46.3	14.3	32.7	10
hHL(m) + Ag	51.4	13.8	28.6	6.2
pHL(w) + Ag	54.1	14.3	26.4	5.2
hHL(s) + Ag	44.1	14.2	35.6	6.1

into the concentration of the functional groups that can occur before and after Ag adsorption, we performed a curve fitting procedure of carbon C1*s* peak (spectra not shown here). As a result of the fitting procedure of all C1*s* spectra, we obtained the following: The major C1 peak at ~285 eV corresponds to the C–C and C–H bond, the second C2 peak at ~286.5 eV is due to the C–OH or C–O–C bond, C3 peak situated at ~288.0 eV corresponds to C=O bond, and the last C4 corresponds to O–C=O bond at 289.5 eV. The quantitative results are summarized in Tables 5 and 6.

It should be mentioned here that there is no trend of changing the data, listed in Table 6, as a result of Ag^+ adsorption. The concentrations of hydroxyl C–OH and carboxyl functional groups are increased after Ag adsorption in comparison with the initial materials.

The Ag 3*d* photoelectron spectra of all studied Ag-modified organics are presented in Fig. 4. Usually, the binding energy of $Ag3d_{5/2}$ is most commonly used for indication of the existence of Ag. Nevertheless, the oxidation state of the silver is rather difficult to be assessed based on its XPS peaks due to very small chemical shifts. For the Ag(0) metallic state, the binding energy of $Ag3d_{5/2}$ is at 368.2 ± 0.1 eV. The binding energy of Ag_2O $3d_{5/2}$ is reported to have a −0.3 eV (negative) shift, while the signal of the other oxide, AgO, shifts by −0.8 eV (also a negative shift).

Our XPS results show that the $Ag3d_{5/2}$ peak has binding energy at about 368.6 eV for all examined adsorbents except for lignin, where this peak is situated at 369.5 eV and can be attributed to the "charge transfer states" discussed in some reports (Huang et al. 2007). Positive core-level shifts for $Ag3d_{5/2}$ have also been reported for extremely small Ag particles approaching 2 nm in diameter (Link and El-Sayed 1999). Although the evaluated binding energy is a little bit higher than the one reported in the literature, we associate it with the presence of Ag in metallic state over the examined adsorbents as it was observed by Herrera et al. (2003) using alfalfa biomass.

The O1*s* peak from the studied adsorbents is also given (Fig. 4). Only two components at 532.0 and 533.5 eV are needed to fit the O1*s* peaks for all studied adsorbents. The two components can be assigned to the existence of organic groups such as C=O and C–O/C–OH, respectively, but not to Ag_2O (528.5–529.3 eV) or AgO (529.2–530.9 eV).

The XPS and EPR results confirm the complex character of the adsorption of Ag^+ ions onto the hydrolyzed waste lignocellulosic materials, and they prove the formation of metallic Ag clusters on the surface of all studied materials. As it is seen from the order concerning the amount of adsorbed Ag^+ ions (5), the procedures for sample preparation (steam explosion or hydrothermal treatment) do not influence the adsorption efficiency.

According to the obtained results, the adsorption of Ag^+ ions passes through several stages. The final stage (EPR and XPS results) is the formation of Ag^0. EPR spectra prove also the formation of clusters of the type Ag_y^{x+}. Hence, the adsorption of Ag^+ ions passes through the following stages:

$$\mathrm{Ag^+(solution)—Ag^+(adsorbate)—}g_y^{x+}\mathrm{(adsorbate)} \\ \mathrm{—Ag^0(adsorbate)} \quad (8)$$

The results of the kinetic studies show that more than one silver ion is involved in the rate-limiting stage of the adsorption process. Therefore, we can assume that the rate of adsorption is determined by the following stage:

$$\mathrm{Ag^+(adsorbate)} \rightarrow \mathrm{Ag}_y^{x+}\mathrm{(adsorbate)} \quad (9)$$

During the stage Ag^+(solution)—Ag^+(adsorbate), an increase in the concentration of H^+ ions occurs, because a

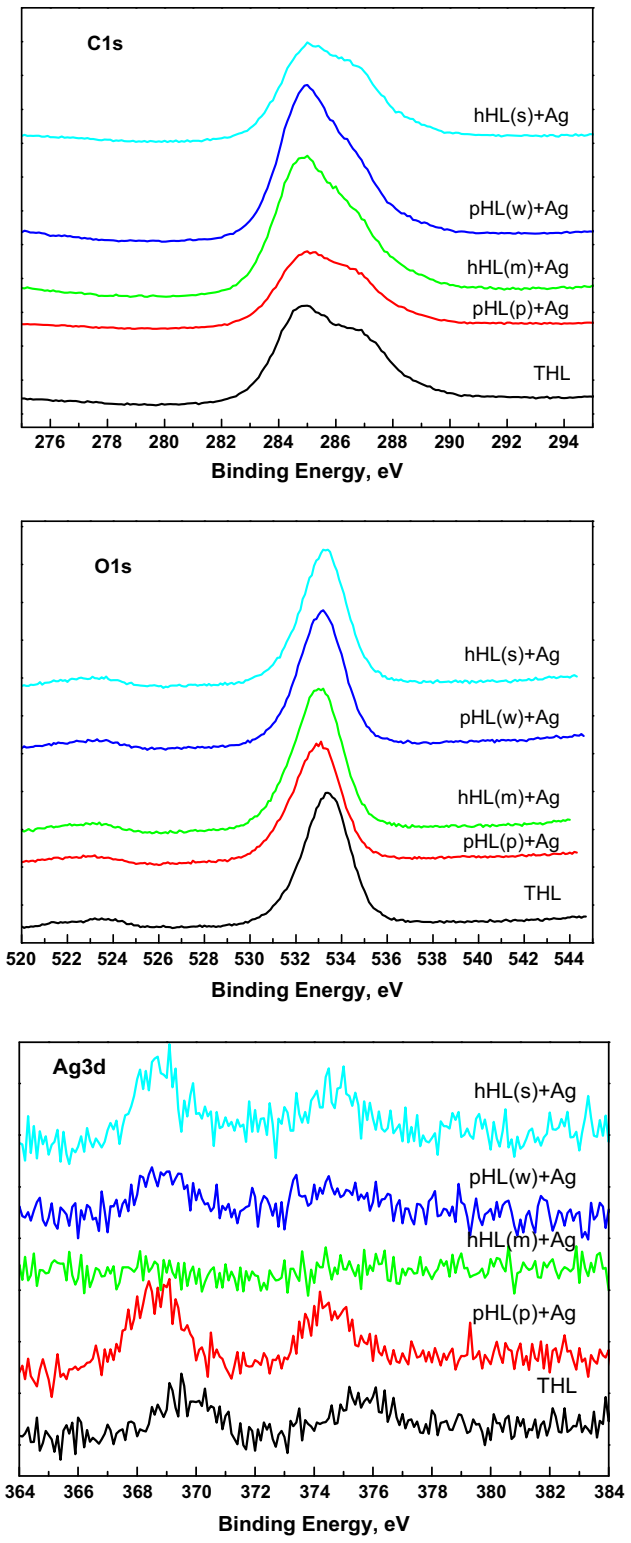

Fig. 4 Photoelectron core level of waste lignocellulosic materials after adsorption of Ag ions for C1*s*, O1*s* and Ag3*d*

decrease in the pH value of the final solutions is observed. Probably, it is due to ion exchange between Ag^+ ions and H^+ of the OH-groups, which facilitates the formation of clusters of the type Ag_y^{x+} in the next stage. The reduction in the silver ions during the last stage Ag_y^{x+}(adsorbate)—Ag^0(adsorbate) causes a release of OH-groups, and their concentration increases (Table 6, XPS-data) as a result of the adsorption.

Conclusion

The adsorption of Ag^+ ions on hydrolyzed waste lignocellulosic materials was studied in the present paper. The influence of the acidity of the initial metal ion solutions on their adsorption was investigated, and the optimal pH range was found out to be about 5.0. The adsorption equilibrium is established within 15 min. The pseudo-second-order kinetic model showed best correlation with experimental data. It was established that both Langmuir and Freundlich types of isotherms described the adsorption process. The adsorption mechanism was investigated, and it was proved that the adsorption of Ag^+ ions passes through several stages. The final stage is the formation of metallic Ag^0. It is assumed that the rate-limiting step of the adsorption process is the formation of clusters of the type Ag_y^{x+}. All investigated materials could be used as promising adsorbents for Ag^+ ions, as well as for preparation of silver-modified catalytic materials for removal of toxic substances from physiologic solutions.

Acknowledgments The authors wish to thank the National Centre for New Materials UNION (Contract No. DCVP-02/2/2009) for the financial support.

References

Ahmedna M, Marshell W, Rao R (2000) Production of granular activated carbons from select agricultural by-products and evaluation of their physical, chemical and adsorption properties. Bioresour Technol 71:113–123

Aksu Z, Kabasakal E (2004) Batch adsorption of 2,4-dichlorophenoxy-acetic acid (2,4-D) from aqueous solution by granular activated carbon. Sep Purif Technol 35:223–240

Ali I (2010) The quest for active carbon adsorbent substitutes: inexpensive adsorbents for toxic metal ions removal from wastewater. Sep Purif Rev 39:95–171

Ali I, Gupta VK (2007) Advances in water treatment by adsorption technology. Nat Protoc 1:2661–2667

Ali I, Asim M, Khan TA (2012) Low cost adsorbents for the removal of organic pollutants from wastewater. J Environ Manag 113:170–183

Allen S, McKay G, Khader K (1989) Intra-particle diffusion of a basic dye during adsorption onto sphagnum peat. Environ Pollut 56:39–50

Angelova D, Uzunov I, Uzunova S, Gigova A, Minchev L (2011) Kinetics of oil and oil products adsorption by carbonized rice husks. Chem Eng J 172:306–311

Baldansuren A, Roduner E (2009) EPR experiments of Ag species supported on NA. Chem Phys Letters 473:135–137

Bukhari IH, Shabbir G, Rehman J, Riaz M, Rasool N, Zubair M, Qu A, Munir S, Shaheen MA (2013) Biosorption of Pb(II), Cu(II) and Mn(II) metal ions from aqueous solutions by using *Typha latifolia* waste biomass. J Environ Prot Ecol 14:453–462

Bumba C, Leonte EP, Dumitrescu C, Ghita I, Stefanescu M (2010) Heavy metals removal using residual fungal biomass. J Environ Prot Ecol 11:822–829

Cao J-G, Li X-M, Ouyang Y, Zheng W, Yang Q (2011) Manganese waste water treatment: biosorption of manganese by Serratia sp. J Environ Prot Ecol 12:661–666

Detcheva A, Vassileva P, Georgieva R (2011) Adsorption of lead onto a silica based nanostructured hybrid material containing aluminium. Compt Rend Acad Bulg Sci 64(6):815–822

Dhabekar B, Menon S, Raja EA, Sanaye SS, Rao TKG, Bhatt BC, Kher RK (2006) ESR and TL mechanism in CaSO4: Ag co-doped phosphors. J Phys D Appl Phys 39:488–2493

Dias J, Alvim-Ferraz M, Almeida M, Rivera-Utrilla J, Sanchez-Polo M (2007) Waste materials for activated carbon preparation and its use in aqueous-phase treatment: a review. J Environ Manage 85:833–846

Foo K, Hamed B (2009) Utilization of rice husk ash as novel adsorbent: a judicious recycling of the colloidal agriculture waste. Adv Colloid Interface Sci 152:39–47

Garcia-Reyes RB, Rangel-Mendez JR, Alfaro-De la Torre MC (2009) Chromium (III) uptake by agro-waste biosorbents: chemical characterization, sorption—desorption studies, and mechanism. J Hazard Mater 30:845–854

Gardea-Torresdey JL, de la Rosa G, Peralta-Videa JR (2004) Use of phytofiltration technologies in the removal of heavy metals: a review. Pure Appl Chem 76:801–813

Guo X, Zhang S, Shan X (2008) Adsorption of metal ions on lignin. J Hazard Mater 151:134–142

Gupta VK, Saleh TA (2013) Sorption of pollutants by porous carbon,carbon nanotubes and fullerene- An overview. Environ Sci Pollut Research 20(5):2828–2843

Gupta VK, Agarwal S, Saleh TA (2011a) Synthesis and characterization of alumina-coated carbon nanotubes and their application for lead removal. J Hazard Mater 185(1):17–23

Gupta VK, Agarwal S, Saleh TA (2011b) Chromium removal by combining the magnetic properties of iron oxide with adsorption properties of carbon nanotubes. Water Res 45(6):2207–2212

Gupta VK, Ali I, Saleh TA, Nayak A, Agarwal S (2012) Chemical treatment technologies for waste-water recycling—an overview. RSC Adv 2:6380–6388

Gupta VK, Rajeev K, Nayak A, Saleh TA, Barakat MA (2013) Adsorptive removal of dyes from aqueous solution onto carbon. Adv Colloid Interface Sci 193:24–34

Herrera I, Gardea-Torresdey JL, Tiemann KJ, Peralta-Videa JR, Armendariz V, Parsons JG (2003) Binding of silver(i) ions by alfalfa biomass (medicago Sativa): batch pH, time, temperature, and ionic strength studies. J Hazard Subst Res 4(1):1–16

Ho Y, Mckay G (1999) Pseudo-second order model for sorption processes. Process Biochem 34:451–465

Huang X, Jain PK, El-Sayed IH, El-Sayed MA (2007) Gold nanoparticles: interesting optical properties and recent applications in cancer diagnostics and therapy. Nanomedicine (Lond) 2:681–693

Ioannidou O, Zabaniotou A (2007) Agricultural residues as precursors for activated carbon production—a review. Renew Sustain Energy Rev 11:1996–2005

Krishnani K, Meng X, Dupont L (2009) Metal ions binding onto lignocellulosic biosorbent. J Environ Sci Health A Tox Hazard Subst Environ Eng 44:688–699

Leinonen H, Letho J (2001) Purification of metal finishing waste waters with zeolites and activated carbons. Waste Manag Res 19:45–57

Link S, El-Sayed MA (1999) Spectral properties and relaxation dynamics of surface plasmon electronic oscillations in gold and silver nanodots and nanorods. J Phys Chem B 103:8410–8426

Liu X, Zhu H, Qin C, Zhou J, Zhao JR, Wang S (2013) Adsorption of heavy metal ion from aqueous single metal solution by aminated epoxy-lignin. BioRes 8:2257–2269

Nameni M, Alavi-Moghadam M, Arami M (2008) Adsorption of Hexavalent Chromium from Aqueous solutions by Wheat bran. Int J Environ Sci Tech 5(2):161–168

Ngah W, Hanafiah M (2008) Removal of heavy metal ions from wastewater by chemically modified plant wastes as adsorbents: a review. Bioresour Technol 99:3935–3948

Obolenskaya AV, Sheglov VP, Akim GL, Akim EL, Kossovich NL, Emelianova IZ (1965) Practical training works in wood and cellulose chemistry. Lesnaya promishlennost, Moscow, pp 411–420 **(in Russian)**

Radoykova T, Dizhbite T, Dobele G, Nenkova S, Valchev I (2013) Characterization of hydrolysed lignocellulosic materials for energy utilization. In: Proceedings of 9th international conference on polysaccharides-glycoscience, 06–08 Nov, Prague, Czech Republic, pp 200–204

Radoykova T, Dimitrova S, Aleksieva I, Nenkova S, Valchev I, Mehandjiev D (2015) Comparative Mn^{2+} adsorption on waste lignocellulosic materials. J Environ Prot Ecol 16:23–32

Rida K, Bouraoui S, Hadnine S (2013) Adsorption of methylene blue from aqueous solution by kaolin and zeolite. Appl Clay Sci 83–84:99–105

Saleh TA (2011) The influence of treatment temperature on the acidity of MWCNT oxidized by HNO_3 or a mixture of HNO_3/H_2SO_4. Appl Surf Sci 257:7746–7751

Saleh TA (2015a) Isotherm, kinetic, and thermodynamic studies on Hg(II) adsorption from aqueous solution by silica-multiwall carbon nanotubes. Environ Sci Pollut Res 22:16721–16731

Saleh TA (2015b) Mercury sorption by silica/carbon nanotubes and silica/activated carbon: a comparison study. J Water Supply Res T 64:892–903

Saleh TA, Gupta VK (2012) Column with CNT/magnesium oxide composite for lead(II) removal from water. Environ Sci Pollut Res 19:1224–1228

Saleh TA, Gupta VK (2014) Processing methods, characteristics and adsorption behavior of tire derived carbons: a review. Adv Colloid Interface Sci 211:93–101

Saleh TA, Agarwal S, Gupta VK (2011) Synthesis of MWCNT/MnO_2 and their application for simultaneous oxidation of arsenite and sorption of arsenate. Appl Catal B Environ 10:46–53

Shinogi Y, Kanri Y (2003) Pyrolysis of plant, animal and human waste: physical and chemical characterization of the pyrolytic products. Bioresour Technol 90:241–247

Sumathi KMS, Mahimairaja S, Naidu R (2005) Use of low-cost biological wastes and vermiculite for removal of chromium from tannery effluent. Bioresour Technol 96:309–316

Vassileva P, Detcheva A (2010) Adsorption of some transition metal ions [Cu(II), Fe(III), Cr(III) and Au(III)] onto lignite-based activated carbons modified by oxidation. Adsorpt Sci Technol 28:229–242

Vassileva P, Detcheva A (2011) Removal of toxic ions from aqueous solutions using lignite-coal-based activated carbons modified by oxidation. Int J Coal Prep Util 31:242–257

Vassileva P, Detcheva A, Uzunov I, Uzunova S (2013) Removal of (some) metal ions from aqueous solutions using pyrolysed rice husks: adsorption kinetics and equilibria. Chem Eng Commun 200:1578–1599

Volesky B (2001) Detoxification of metal-bearing effluents: biosorption for the next century. Hydrometallurgy 59:203–216

Yuvaraja G, Krishnaiah N, Subbaiah MV, Krishnaiah A (2014) Biosorption of Pb(II) from aqueous solution by Solanum melongena leaf powder as a low-cost biosorbent prepared from agricultural waste. Colloids Surf B: Biointerfaces 114:75–81